

*Dedicated to Prof. Bogdan C. Simionescu  
on the occasion of his 75<sup>th</sup> anniversary*

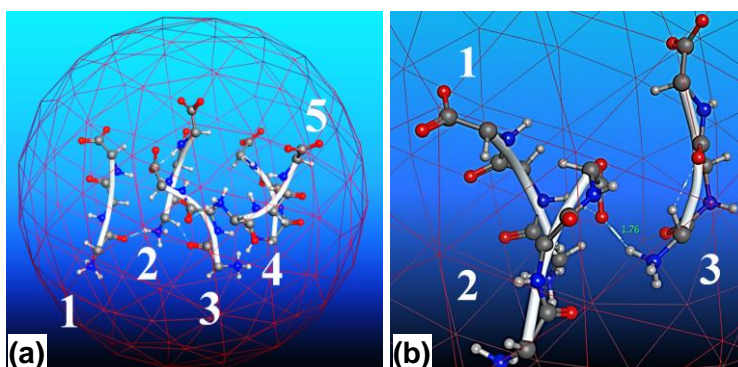
## MASS SPECTROMETRIC CHARACTERIZATION OF SOME GEL-FORMING PEPTIDES

Ștefania-Claudia JITARU and Gabi DROCHIOIU\*

“Al. I. Cuza” University of Iasi, 11 Carol I, RO-6600, Iasi, Roumania

*Received November 15, 2022*

Peptide-based hydrogels have become an area of intense investigation due to their easy design, possibility to make a large range of hierarchical nanostructures and their high biocompatibility and biodegradability. Here, we investigated by mass spectrometry (MS) a few synthetic gel-forming peptides having different amino acid sequences. Four different peptides were selected for MS measurements: EEE-OH, FFFFF-OH, FESNF-NH<sub>2</sub>, and LWMRFA-OH. Our data show that mass spectrometry can be used to get detailed information on structure, molecular weight, and chemical bond energies of gel-forming peptides as well as to assess their purity and stability. Fourier transform infrared spectroscopy (FTIR) and theoretical studies carried out using GPMW and ChemDraw Ultra computer programs confirmed the MS data. The peptide tendency to aggregate, a process observed by MS in the case of peptide EEE in a polar environment, was also theoretically investigated by molecular modeling.



### INTRODUCTION

Peptide chemistry has become an important research area in the study of natural compounds.<sup>1,2</sup> In addition, peptide-based hydrogels have received much attention because of their possible biomedical applications.<sup>3–6</sup> Fortunately, large amounts of peptides can be easily produced by solid-phase peptide synthesis (SPPS), widely based on Fmoc/tBu strategy.<sup>7,8</sup> Most of the gel forming peptides have a  $\beta$ -sheet motif that is composed of alternating hydrophobic and hydrophilic amino acids.<sup>5</sup> Indeed,

the propensity of peptides to assemble into polymorphic fibrils suggests that cross- $\beta$  fibrils comprising hydrogels may also be polymorphic.<sup>9,10</sup> This biological motif, the  $\beta$ -sheet peptide, can be exploited in designed oligopeptides that self-assemble into polymeric tapes and with potentially useful mechanical properties.<sup>11</sup> Therefore, the relationship between peptide design, resulting conformation and morphological properties of the self-assembled peptide was recently reviewed.<sup>12</sup> For instance, the EEE sequence (E = glutamic acid residue) provides the necessary hydrophilic/

\* Corresponding author: gabidr@uaic.ro

hydrophobic balance to achieve amphiphilicity.<sup>13</sup> Glutamic acid peptides form negatively-charged self-assembling amphiphilic molecules involved in calcium phosphate mineralization.<sup>14</sup> Many other peptides, such as phenylalanyl peptides, have the ability to self-assemble to form hydrogels.<sup>15</sup> Fmoc protected aromatic amino acids can also form hydrogels.<sup>16</sup> Some Fmoc-dipeptides can self-assemble due to the protective Fmoc group bound to the amino group of amino acids containing an alkyl or aromatic residue with high hydrophobicity (like phenylalanine or leucine).<sup>17</sup>

Molecular self-assembly is a spontaneous process when molecules are organized into well-defined nanostructures, governed by weak non-covalent bonds, such as electrostatic interactions, water-mediated or classical hydrogen bonds, hydrophobic and hydrophilic interactions van der Waals interactions.<sup>18–20</sup> Phenylalanine alone possesses self-assembling properties that may induce globular protein aggregation of physiological importance to the patients with phenylketonuria.<sup>21</sup> Fmoc protected aromatic amino acids have also the capacity to form hydrogels.<sup>16</sup> The phenylalanine (F) and tryptophan (W) residues facilitate aggregation, but the contribution of serine (S) or threonine (T) cannot be neglected.<sup>22</sup>

It is well-known that lysozyme found in the hen egg white is a typical protein with amyloid and aggregation properties.<sup>23,24</sup> Moreover, its sequence,<sup>34</sup> FESNF<sup>38</sup>, contains F and E residues, which are specific to gel-forming peptides.<sup>25</sup> Therefore, a peptide with FESNF sequence of lysozyme was synthesized and investigated in this work in comparison with the glutamic-rich peptide (EEE) and phenylalanine-rich peptide (FFFFF).

The investigation of the stoichiometry, specificity and fragmentation mechanisms of peptides and complexes and aggregates can be done by mass spectrometry (MS) and tandem mass spectrometry (MS/MS).<sup>26</sup> Therefore, the purpose of this work is the characterization by MS of a few peptides with potential self-assembly properties and possible biomedical implications. In addition, because the peptides can undergo degradation over time by fragmentation, their purity should be known. Mass spectrometry can also evaluate the purity of peptides before they are introduced into experiments. Besides, a hexapeptide, LWMRFA (Leu-Trp-Met-Arg-Phe-Ala) was also investigated here as a model peptide. Therefore, investigating these four peptides allows us to better understand the fragmentation mechanisms in mass spectrometry experiments. The theoretical investigations were carried out using GPMaw and ChemDraw Ultra computer programs. Molecular

modelling was performed on the EEE peptide using the droplet method, and the results will be reported in another paper to simplify this work.

## RESULTS AND DISCUSSION

### Investigation of the EEE peptide

The EEE peptide (glutamyl-glutamyl-glutamic acid) has been stored for a long time, and therefore, in addition to its  $m/z = 406.1$  peak, many other signals attributed to impurities were present in its ESI ion trap mass spectrum (Fig. 1a). Under storage conditions, the EEE peptide underwent loss of one water molecule, with probable formation of a peptide containing a pyroglutamic acid residue, which shows a characteristic peak at  $m/z = 387.7$ . The relatively high intensity of this peak suggests that the peptide has been stored at high temperatures, such as those in the laboratory, for a sufficiently long period of time. The presence of the signal at  $m/z = 148.0$ , attributed to the  $\gamma_1^+$  fragment, indicated the fragmentation of the peptide molecule with the removal of the remaining glutamic acid from the C-terminus. A certain proportion, which can be estimated at about 20–25% of the peptide molecules were found in the form of dimers ( $[2M + H]^+$ ,  $m/z = 811.2$ ). The peak found at  $m/z = 371.5$  would suggest the loss of two water molecules by the peptide molecule, with the formation of a peptide containing two pyroglutamic acid residues. Therefore, the ESI mass spectrum has the ability to identify changes in peptides during storage, as well as to determine their purity.

After purification by RP-HPLC, the MS spectrum was found to be simplified, but the dimer signal increased unexpectedly (Fig. 1b). The molecular ion of the EEE-OH peptide ( $[M + H]^+$ ) showed a relatively weak peak at  $m/z = 406.1$ . At the same time, the peak intensity of the peptide obtained by removing a water molecule was even lower ( $[M - H_2O + H]^+$ ;  $m/z = 388.2$ ). The fragmentation process in negative mode of the dimer of EEE-OH peptide also produced surprising results (Figs. 1c and d). Thus, the dimer was only partially cleaved into the individual molecules of the peptide, while a new dimer was formed by removing a molecule of water. It was found at  $m/z = 792.1$ . A condensation reaction is likely to take place to form a new molecule by removing water. These data also suggest the high stability of the dimer formed after purification. At the same time, its stability decreased over time, as shown in Fig. 1a.

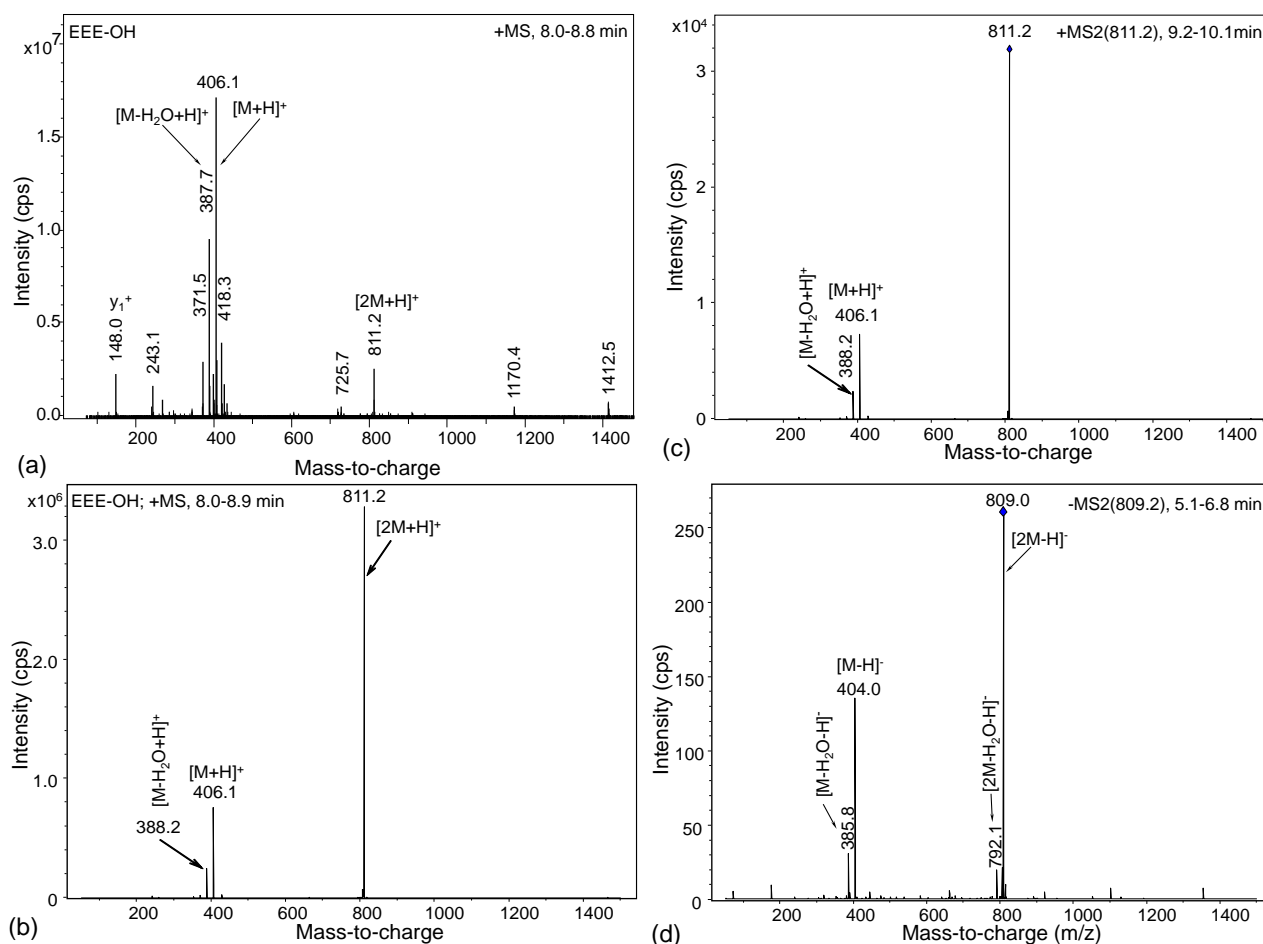


Fig. 1 – ESI ion trap mass spectra of glutamyl-glutamyl-glutamic acid peptide (EEE-OH): (a) positive-mode mass spectrum of EEE-OH peptide after long-term storage; (b) mass spectrum of EEE-OH peptide after purification by RP-HPLC; (c) positive mode tandem mass spectrum of EEE-OH peptide; (d) negative mode tandem mass spectrum of EEE-OH peptide.

As expected, the peptide negative molecular ion,  $[M-H]^-$ , even of lower intensity as compared with that of dimer, was identified at  $m/z = 404.0$ , whereas the molecule formed by water removal was identified at  $m/z = 385.8$ .

The peptide secondary structure was investigated by infrared spectroscopy.<sup>27</sup> The FTIR spectrum of the EEE peptide also suggests peptide aggregation, as an absorption band around  $1610\text{ cm}^{-1}$  was found (Fig. 2). In fact, the second derivative of the FTIR spectrum has confirmed our supposition (a negative maximum at  $1614\text{ cm}^{-1}$  was noticed, which was assigned to the aggregation process). The large absorption band at  $3433\text{ cm}^{-1}$  is characteristic to amino and carboxyl groups. In addition, an absorption band at  $1633\text{ cm}^{-1}$  and another one at  $1674\text{ cm}^{-1}$  is typically observed when  $\beta$ -sheets are dominant.<sup>27</sup> Indeed, upon gelation, the absorption peaks at  $1622\text{ cm}^{-1}$  and  $1674\text{ cm}^{-1}$  are present, indicative of a  $\beta$ -sheet structure.

The process of dimerization of peptide EEE was observed when two molecules were studied by

molecular dynamic simulation (a larger discussion will be given in another paper). The same characteristics were observed when four and five EEE peptide molecules were analyzed (not shown). Thus, the first two peptides were found to be more closely related than the other two peptides in the group of four analyzed. As a result, in this case two dimers appeared.

The main interactions possibly take place between glutamic acid residues via the oxygen atoms and hydrogen atoms in the amino group. In the case of two peptide interaction, hydrogen bonds are generated involving the oxygen atoms of Glu residue and water molecules. Furthermore, due to the structural limitation of the peptide, the polarity of the molecule intervenes in the dimerization process as a consequence of sequence similarity.

While searching the literature, we found that the EEE sequence has been introduced into the molecule of other peptides or organic compounds.<sup>28</sup> However, we did not find a study on EEE peptide dimerization.

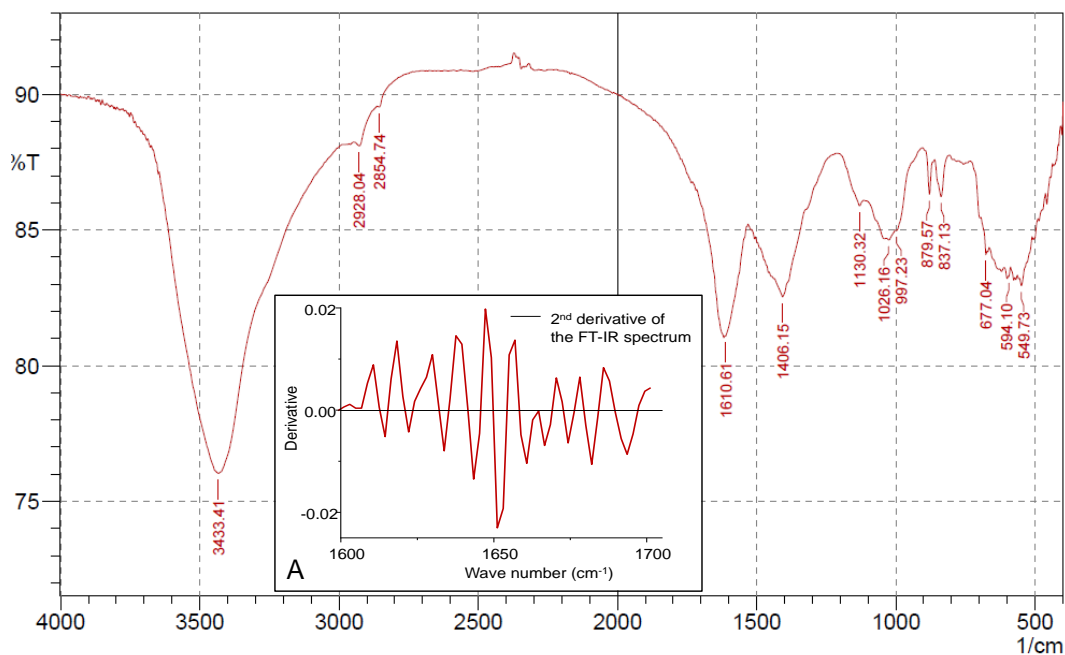


Fig. 2 – FTIR spectrum of EEE peptide and its second derivative (Insert A).

### The FFFFF peptide

The less-hydrophobic-and-low-pI peptides, including FFFFF show also low cellular uptake.<sup>29</sup> We have investigated here the hydrophobicity and pI value of this peptide. Here, we investigate the purity and structure of peptide FFFFF-OH, as well as its cleavage during the MS/MS process (Fig. 3). Figure 3a indicated the presence of many impurities associated with peptide. These impurities appeared at  $m/z = 768.3$  (molecular weight,  $M+15$  Da),  $m/z = 1170.5$ , and  $m/z = 1412.6$ , which suggests that they are not peptide fragments. We searched for peptide fragments below  $m/z = 754.3$ , and noticed that the signals at  $m/z = 243.1$ ,  $m/z = 371.3$ ,  $399.4$ , and  $m/z = 427.4$  are not present in the MS/MS fragmentation table inserted in Fig. 3d. Therefore, these results suggest that the peptide was not pure and it was necessary to verify the purity of the peptide by MS before a new experiment. In addition, Fig. 3a also showed that the peptide FFFFF does not cleave during storage. Moreover, we did not observe by MS any tendency of dimerization of this peptide.

Figure 3b shows the MS/MS fragments and thus confirms the primary structure of peptide FFFFF-OH. The most prominent peaks belong to  $b_3^+$  and  $b_4^+$ , which suggest that these fragments are more stable than the  $y$ -type fragments, probably due to the presence of amino groups at N-terminus. Thus, the formation of  $b_3^+$  and  $y_2^+$  assumes the cleavage between the third and the fourth phenylalanine residues, but the positive charge

remains on the  $b$ -type fragment. The peak at  $m/z = 763.3$  was assigned to peptide molecule which lost a molecule of water. The same water-lost peptide also appeared at  $m/z = 369.2$  as double charged fragment ion. This denotes a relative high stability of peptide and its capability to form a cyclic structure by eliminating a water molecule (Fig. 4d). However, we do not exclude the formation of a linear structure as shown in Scheme 1. Therefore, a linear structure of the molecular ion shown in Fig. 4d is even more likely, since an amino group is free and can accommodate a proton to form a double-exchanged molecular ion.

It is worth to see the formation of  $a$ -type fragments such as  $a_2^+$  and  $a_4^+$ , as well as  $[a_4-NH_3]^+$ , suggesting the high stability of  $FF^+$  or  $FFFF^+$  fragments after elimination of C=O group or even C=O and  $NH_3$  groups. Consequently, Fig. 3c shows the possible structure of the fragment seen at  $m/z = 544.2$  in the MS/MS spectrum.

Therefore, the fragmentation of peptide FFFFF-OH during the MS/MS process results mostly in the formation of  $b$ -type fragments,  $b_3^+$  being of the highest intensity ( $m/z = 442.2$  and  $m/z = 589.2$ ), which showed molecule splitting into two fragments: FFF and FF. However, the other splitting patterns demonstrated that the peptide molecule is rather stable and other fragmentations are also possible. Figure 4 also shows the formation of various peptide fragments in the MS/MS process. All these fragments suggest the complex fragmentation process of such a simple peptide molecule.

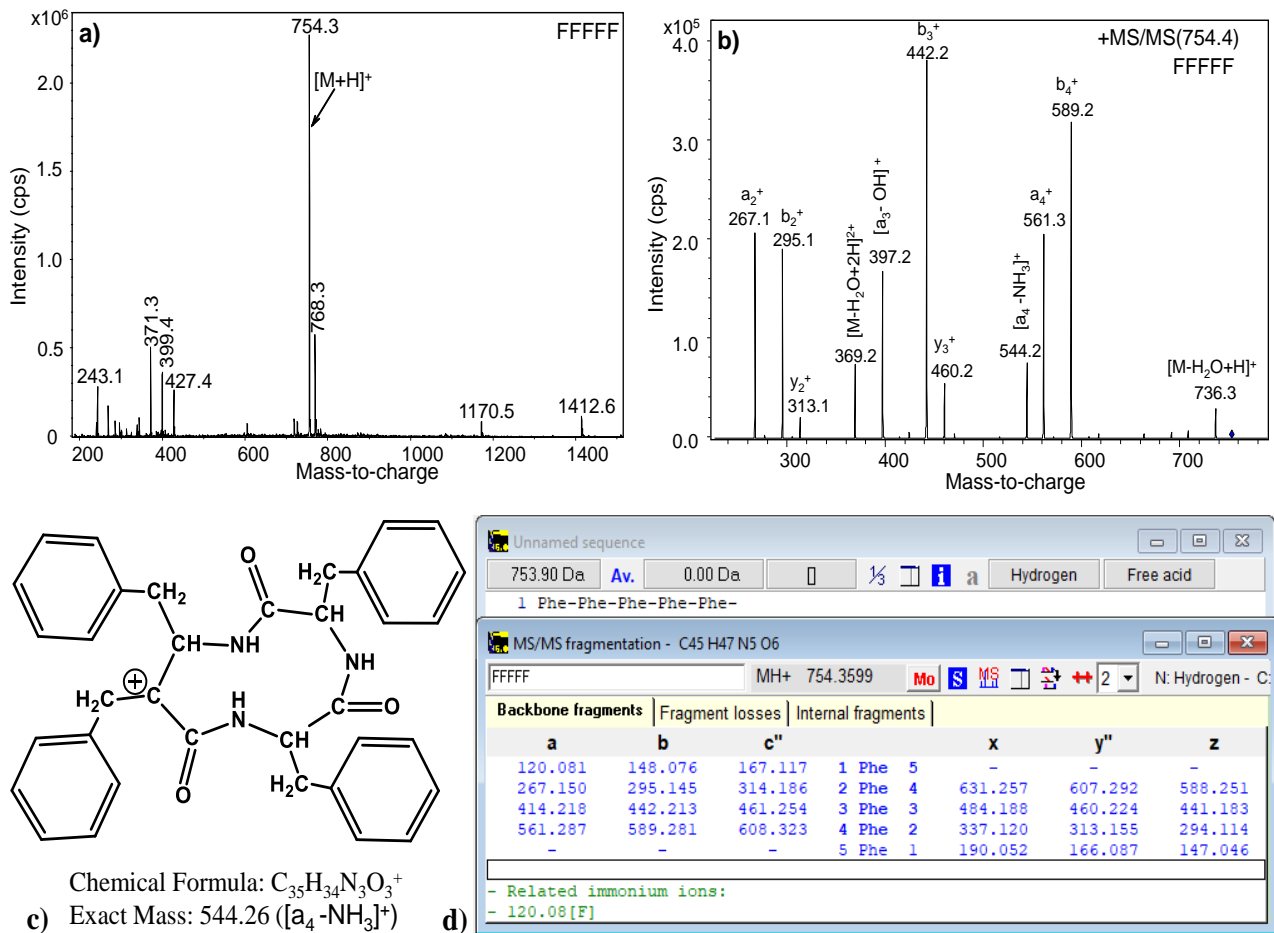
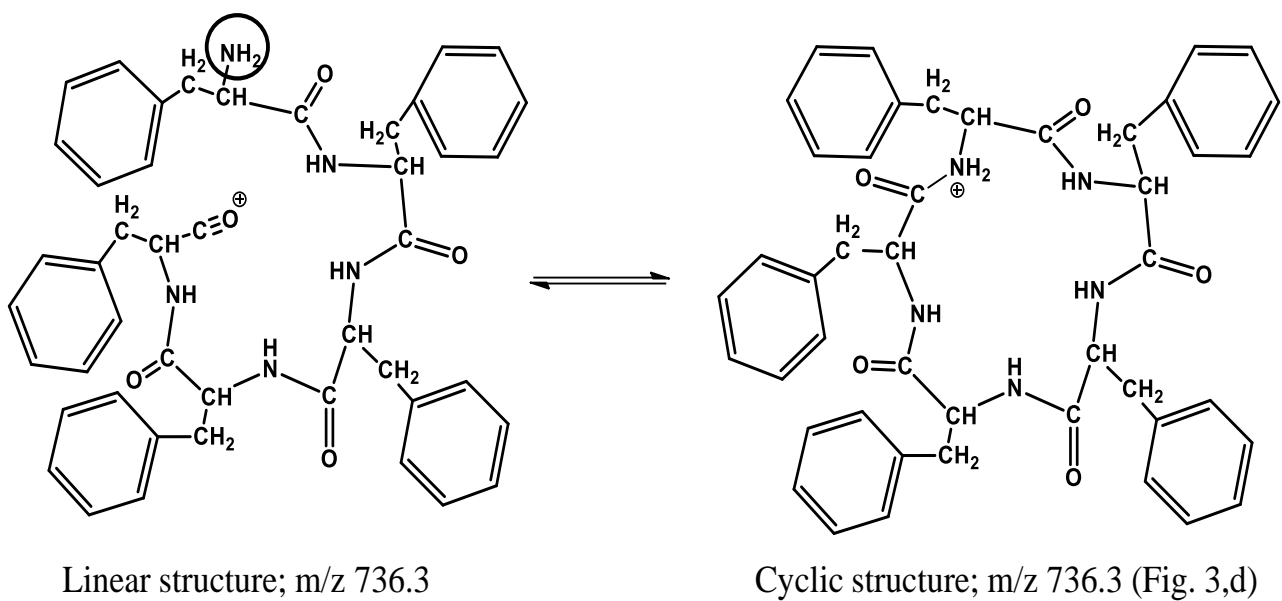


Fig. 3 – The ESI ion trap mass spectra of peptide FFFFF-OH: (a) positive-mode mass spectrum of peptide FFFFF-OH; (b) positive mode tandem MS/MS spectrum of peptide FFFFF-OH; (c) proposed structure of the molecular ion at  $m/z = 544.2$  in the MS/MS spectrum; (d) list of positive fragments of peptide FFFFF-OH resulted in the MS/MS process.



Scheme 1 – Possible structures of the molecular ion at  $m/z = 736.3$  (C<sub>45</sub>H<sub>46</sub>N<sub>5</sub>O<sub>5</sub><sup>+</sup>; Exact Mass: 736.35; Molecular Weight: 736.88).

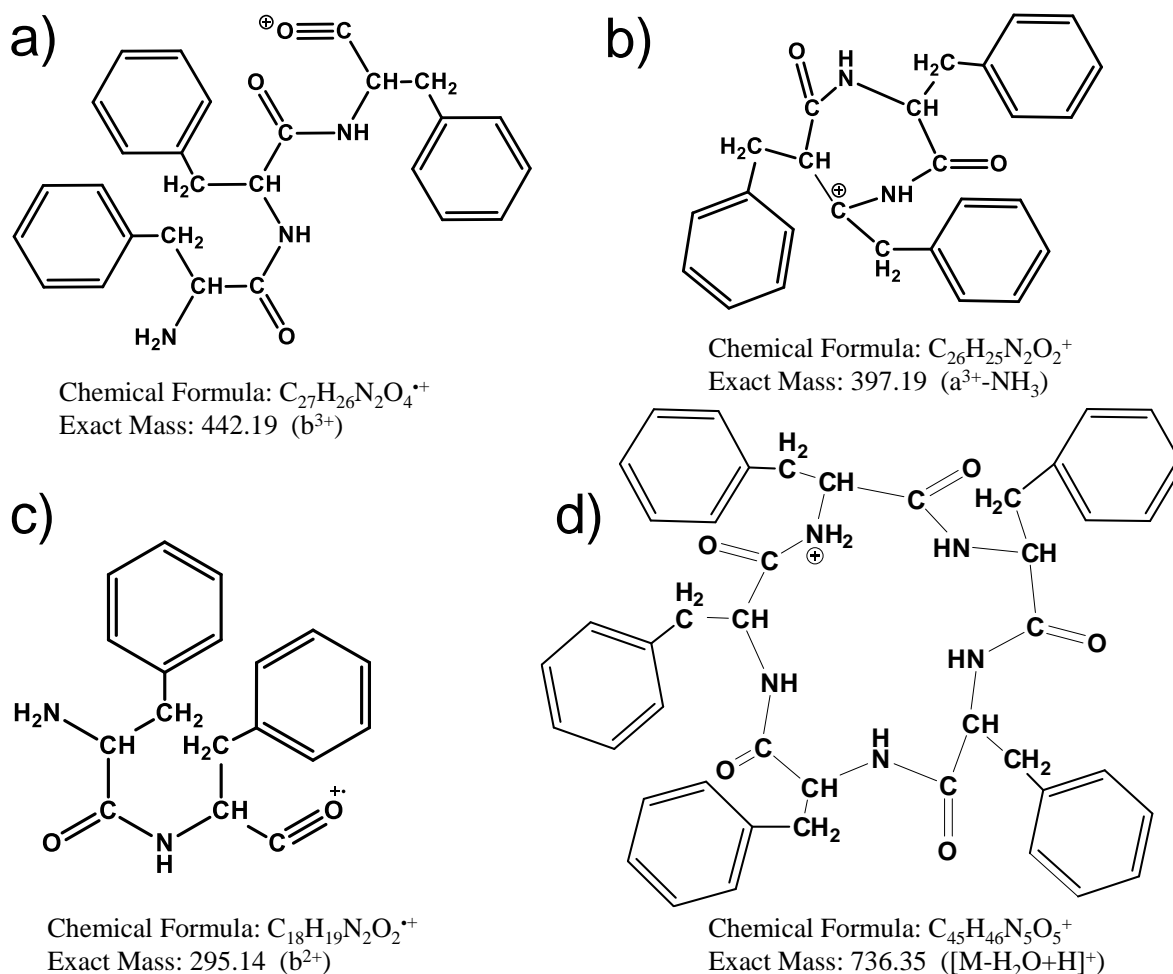


Fig. 4 – Possible structures of some molecular ions identified in the MS/MS spectrum of the FFFFF-OH peptide: (a) The  $b^{3+}$  fragment at  $m/z = 442.2$ ; (b) the  $a^{3+}$  fragment loses a  $NH_3$  molecule to form a positive-charged molecular ion at  $m/z = 397.2$ ; (c) the expected  $b^{2+}$  fragment ion, which is visible at  $m/z = 295.1$ ; (d) the proposed cyclic structure of the peptide molecule after water elimination.

### The gel-forming peptide FESNF-NH<sub>2</sub>

The amidated FESNF-NH<sub>2</sub> peptide was synthesized by Fmoc/tBu strategy of solid phase peptide synthesis (SPPS), which consists in the activation of the carboxyl groups by aminium-derived coupling reagents on PEG-modified polystyrene resins.<sup>8</sup> The crude peptide mixture was then purified by RP-HPLC (Fig. 5). The chromatograms were registered at three wavelength values: 215 nm, 220 nm and 255 nm. Because of its high intensity, we show here only the spectrum recorded at 215 nm wavelength. However, the main peak in the chromatogram, found at a retention time of 11.64 min, was accompanied by another peak at 13.96 min, suggesting that a protective group was not completely removed. Nevertheless, we succeeded to separate the two compounds, so that the desired peptide was obtained in pure state.

The raw mixtures, resulted after solid phase synthesis, were analyzed by mass spectrometry prior to HPLC separation in order to confirm the presence of desired peptides. Thus, the compounds which appeared as two main peaks in the RP-HPLC chromatogram (Fig. 5) were collected and analyzed by MALDI-TOF mass spectrometry using DHB as matrix. The main spectrometric results were presented elsewhere.<sup>30</sup> The MALDI-ToF spectrum of the compound with the characteristic peak at 11.64 min retention time confirmed a molecular weight of 642.5 Da, characteristic to the molecular ion  $[M+H]^+$ , where M is molecular weight of protonated peptide FESNF-NH<sub>2</sub> (not shown). Other molecular ions, such as  $[M+Na]^+$  and  $[M+K]^+$  were found at  $m/z = 664.5$  and  $680.4$ , respectively (their intensity was 50% and 30%, respectively, of the intensity of free peptide peak). The peak eluting at 13.96 min in the chromatogram was attributed

to the molecular ion  $[M + 106 + H]^+$  and its sodium and potassium adducts, which appeared at  $m/z = 748.8$  (assigned to  $[M + 106 + H]^+$ ),  $m/z = 770.7$  (assigned to  $[M + 106 + Na]^+$ ), and  $m/z = 786.6$  (assigned to  $[M + 106 + K]^+$ ). The intensity of

adducts with sodium and potassium was only about 30% and 15%, respectively, of the intensity of free peptide ( $M+106$ ) peak, suggesting a lower affinity of this compound toward alkaline metal ions.

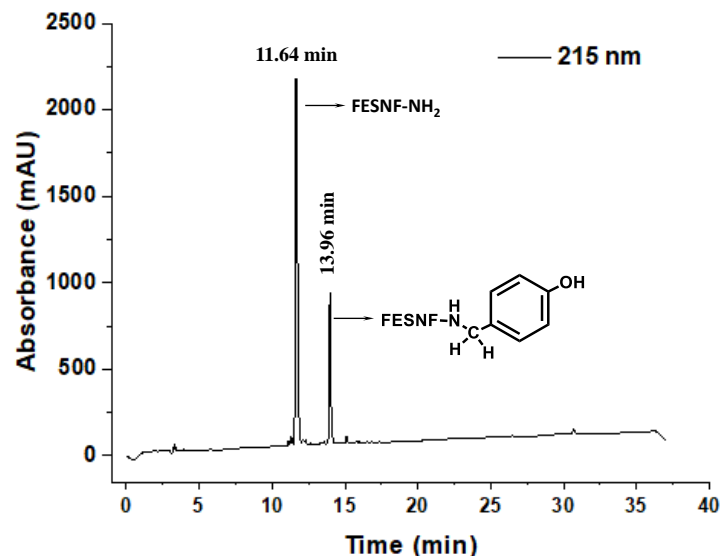
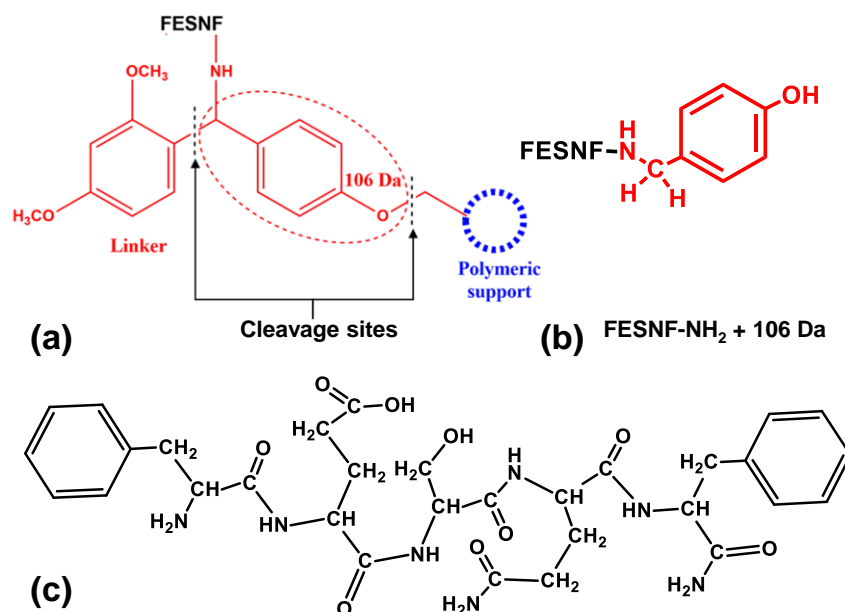


Fig. 5 – RP-HPLC chromatogram of the crude peptide mixture resulted from solid phase synthesis of FESNF-NH<sub>2</sub> sequence.

The difference of 106 Daltons may correspond to a residue in the rink amide linker due to incomplete cleavage, but which increase the hydrophobicity of the resulted molecule. These results are in concordance with previous reported data suggesting a partial cleavage of the A $\beta$  truncated peptide from the resin support.<sup>31</sup> The two molecules were clear separated by RP-HPLC, so that two different compounds were

obtained, a peptide and its conjugate with a radical from the resin linker (Fig. 5). C-terminal N-alkylated peptide amides have also been reported as by-products when using a TIS:TFA:water mixture in the cleavage step. The excess of 106 Da in the mass spectrum can be explained by the inadequate cleavage of the peptide from the rink amide resin as indicated in Scheme 2.



Scheme 2 – Structure of peptide FESNF and its conjugate: (a) inadequate cleavage sites in the peptide-resin complex resulting in a peptide conjugate with a molecular mass higher by 106 Da; (b) proposed structure of peptide conjugate; (c) peptide primary structure.



### The LWMRFA peptide

The relative net charge of the LWMRFA-OH peptide at pH 7.0 was +1, while the MS spectrum suggested the formation of a doubly charged molecular ion,  $[M+2H]^{2+}$ , as the main component.<sup>32</sup> The ESI ion trap MS spectra of peptide LWMRFA indicated the high purity of this peptide (Fig. 6a). The MS/MS spectrum confirmed the peptide sequence, all

9 peptide fragments being identified mostly as *b* and *y* type of fragmentation (Fig. 6b). This spectrum also indicated a weaker bond between the rest of tryptophan and that of methionine, which can break more easily to form the molecular ions  $y_4^+$  (the highest intensity peak) and  $b_2^+$ . In addition, after removal of the leucine residue with the formation of the  $y_5^+$  molecular ion (WMRFA<sup>+</sup>), it can further fragment by breaking up the tryptophan residue.

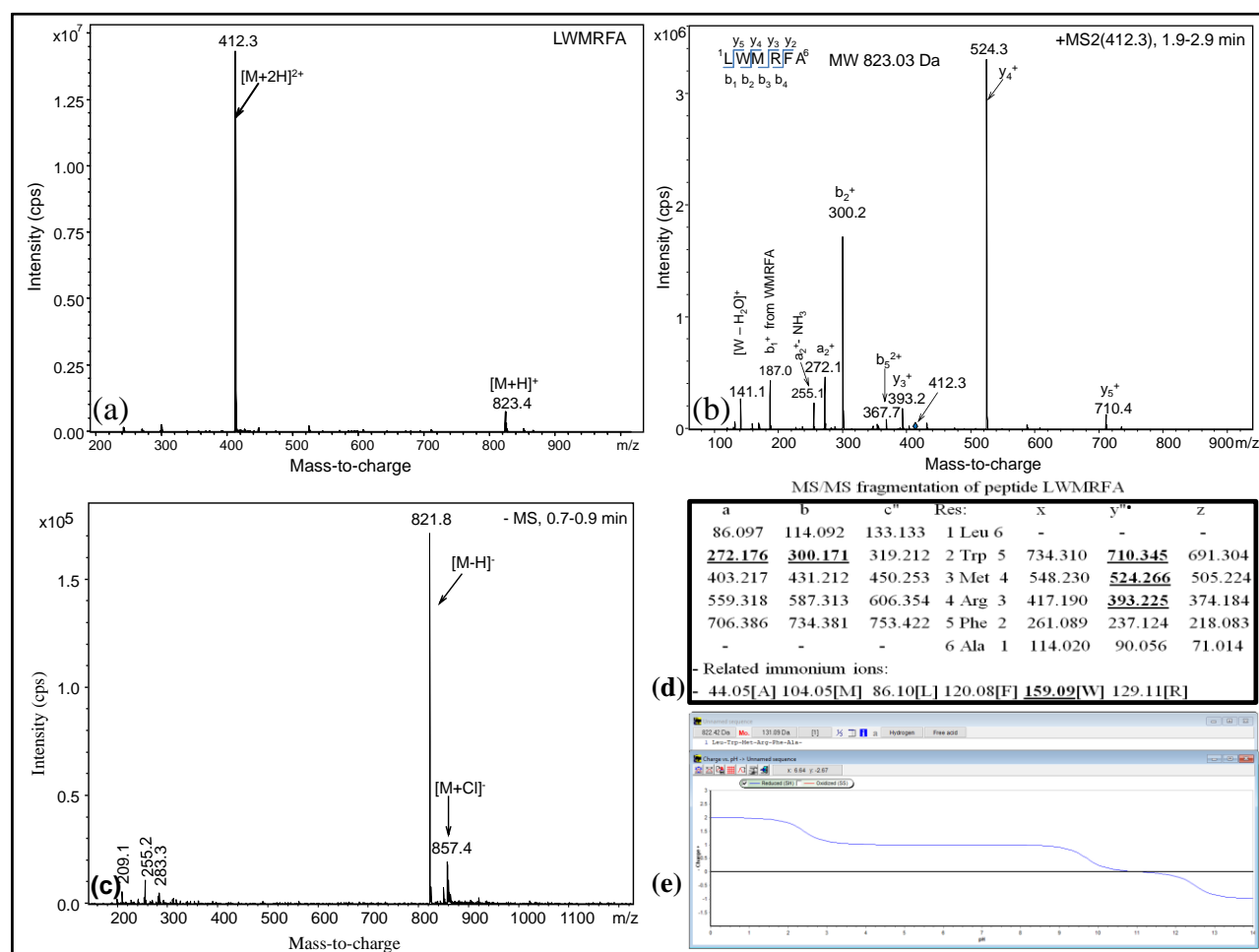


Fig. 6 – ESI-MS LWMRFA. The ESI ion trap MS and tandem MS/MS spectra of peptide LWMRFA: (a) positive mode MS of peptide LWMRFA; (b) MS/MS spectrum of the same peptide; (c) negative mode MS of peptide LWMRFA; (d) list of positive fragments of LWMRFA peptide resulted in the MS/MS process; (e) charge versus pH plot generated by GPMW software.

Even at acidic pH there are positively charged molecular species due to the attachment of protons to peptide molecules and negatively charged species due to the loss of protons from the molecule or the binding of negative ions (*e.g.* Cl<sup>-</sup>).

AChE cleaves the synthetic peptide LWMRFA into LWMR and FA (Novales-Li, 1993).<sup>33</sup> In contrast, the MS/MS spectra of this peptide showed the formation of  $b_2^+$  and  $y_4^+$  molecular ions and therefore the peptide molecule was cleaved into stable LW and MRFA species.

### Discussion

First of all, our research revealed that MS and MS/MS spectra could be used to prove both the purity and structure of newly synthesized peptides. However, we used mass spectrometry to evaluate oligomerization of gel-forming peptides, but no dimerization was observed except for peptide EEE. Therefore, other environmental conditions may enhance the peptide oligomerization process, such as aqueous solutions. In addition, such phenomena



are time-dependent, while MS measurements take a few minutes.

Some  $\beta$ -sheet peptides stabilize integral membrane proteins, whereby they self-assemble in solution as filaments and restructure upon association with those proteins.<sup>34</sup> Therefore, we have also studied the aggregation process by infrared spectroscopy. For instance, a band with the wavelength around  $1615\text{ cm}^{-1}$  could be attributed to the structural changes, which are associated with the presence of aggregates.<sup>35</sup> However, there are short  $\alpha$ -helical peptides that form responsive fibrils and hydrogels at physiological pH and salt.<sup>36</sup>

Recently, a peptide FRSAPFIE-NH<sub>2</sub>, which is a sequence of human collagen, was synthesized and studied by MS and subjected to self-assembling investigations.<sup>37</sup> Based on theoretical calculations, this peptide appears to form a bundle-type association, with a type of fibrillary tangles particle.

It was shown that nanofibers functionalized by EEE sequence enhanced biomineralization process due to osteoinductive properties for differentiation of mesenchymal stem cells.<sup>14</sup> Here, we have also shown the tendency of this peptide to aggregate and form fibrils; it is possible that the EEE peptide and its oligomers bind to Ca<sup>2+</sup> ions, which enhances the fibrillation process.

Initially, the peptide LWMRFA was used as a substrate for proteinase B, when a preferential attack at Arg-Phe and more slowly at Trp-Met of the enzyme was shown.<sup>38</sup> In addition, LWMRFA has been used in the past to prove the triptych activity of acetylcholinesterase (EC 3.1.1.7).<sup>39</sup> However, we introduced this complex peptide into our experiments as a model for investigating peptides by MS. The arginine residue in the peptide molecules may prevent aggregation because of the pI value of the peptide of about 10–11 at pH = 7.0, resulting in an electrical charge capable of repelling individual molecules from each other.

Gel-forming peptides are also implicated in the etiology of diseases such as Alzheimer's disease.<sup>40,41</sup> Previously, replacement of histidine residues in amyloid- $\beta$  peptides with alanine and other amino acids showed an increase in the gelling character of the newly synthesized peptides.<sup>42–45</sup>

## EXPERIMENTAL

### Materials

All reagents were analytical grade, purchased from commercial sources and used as received unless stated otherwise.

The solutions and buffers were prepared with MilliQ-grade water ( $18.2\text{ M}\Omega\cdot\text{cm}$ ) produced by a Milli-Q system (Millipore, USA). NovaSyn TGR resin was from Novabiochem. Protected amino acids needed for peptide synthesis were provided by GL Biochem (Shanghai, China), whereas bromophenol blue, ninhydrin, acetonitrile (ACN, HPLC grade), trifluoroethanol (TFE), and trifluoroacetic acid (TFA) were from Merck. Diethylether, acetic acid and benzotriazole-1-yl-oxy-tris-(dimethylamino)-phosphonium hexafluorophosphate (PyBOP as activator) were obtained from Carl Roth GmbH (Karlsruhe, Germany). Dichloromethane (DCM) was from Scharlau (Spain), whereas triisopropylsilan (TIS), dimethylformamide (DMF), piperidine, 4-methylmorpholine (NMM) and  $\alpha$ -hydroxycinnamic acid (HCCA) were bought from Sigma-Aldrich (UK). Amonium acetate buffer was purchased from (CarlRoth GmbH), while hydrochloric acid (HCl) from Sigma-Aldrich Ltd. The peptide LWMRFA was purchased from Serva Feinbiochem (Heidelberg, Germany), the tripeptide EEE (L- $\alpha$ -glutamyl-L- $\alpha$ -glutamyl-L-glutamic acid) was procured from ChEBI (Cambridge, UK), whereas the pentapeptide FFFFF, from Sigma. All building block amino acids were Fmoc protected (where Fmoc group is 9-fluorenylmethoxycarbonyl). The core amino acids were tertbutyl (tBu) or trityl (Trt) protected. All peptides except the newly synthesized FESNF were stored at 4 °C in the refrigerator for two years prior to experiments to demonstrate their stability over time. Before MS measurements, all peptides were dissolved in 50% TFA (v/v) and used after solvent evaporation.

### Instruments

The electrospray ionization mass spectrometric and tandem MS/MS measurements were carried out on a Bruker Daltonics Esquire 3000plus (Bremen, Germany) ion trap mass spectrometer. Spectra were acquired in the 100–2000  $m/z$  range. The instrument was used both in positive and negative ion mode. Samples were analyzed by direct sample introduction using a syringe pump in a flow rate of 4  $\mu\text{L}/\text{min}$ . The peptides were dissolved in 1:1 acetonitrile: water (v/v) solvent mixture, containing 0.1% acetic acid.

The UV-visible spectra were performed on a Libra S35 PC UV/VIS spectrophotometer with 1 cm matched cells of quartz. The infrared spectra of peptides, after evaporation to dryness, were recorded in solid KBr using a JASCO 660+ FT-IR spectrophotometer (FT-IR Jasco Corporation, 2967-5, Ishikawa-cho, Hachioji, Tokyo 192, Japan), and reported as wavenumbers ( $\text{cm}^{-1}$ ). The synthetic peptides were purified using a Dionex UltiMate 3000 UHPLC system equipped with an autosampler (Thermo Scientific, US). Separation was performed on a Vydac analytical C18 column characterized by 5.0  $\mu\text{m}$  particle size, 4.6 mm inner diameter and 250 mm length. The raw spectral data was processed using Chromeleon™ 7.2 Chromatography Data System (CDS). A polar-organic mobile phase mixture consisted in an aqueous solution of 0.1% TFA in milliQ-grade water (v/v) (solvent A) and a partially aqueous solution of 80% ACN and 0.1% TFA in milliQ-grade water (solvent B). The peptides ( $1\text{ mg mL}^{-1}$ ) were dissolved in solvent A, filtered and automatically injected into the chromatographic system. The separation was performed at a flow rate of 1  $\text{mL}/\text{min}$ , whereas the wavelength values of UV detector were 215 nm, 220 nm and 255 nm, respectively. A temperature of 25 °C was used for the thermostatic column chamber. For a suitable separation the gradient elution was used leading finally to a method with 37 min duration.

The volume of the sample solution injected was 30  $\mu$ L. The gradient used is presented in Table 1.

Table 1

The gradient used for FESNF-NH<sub>2</sub> separation by RP-HPLC

Time (min)	% A eluent	% B eluent
0	95	5
2	95	5
30	0	100
32	0	100
35	95	5
37	95	5

### Peptide synthesis

The solid-phase peptide synthesis (SPPS) of pentapeptide FESNF-NH<sub>2</sub> (Phe-Glu-Ser-Asn-Phe) was manually performed on a Fmoc Rink Amid MBHA Resin (0.48 mmol/g) using a syringe (5 ml) fitted with a sintered glass frit by Fmoc/tBu strategy starting from C- to N-terminus.<sup>46,47</sup> The washing solvents and necessary reagents were removed by suction. Peptide bonds between amino acids were formed by successive stages of deprotection and coupling. A 20% solution of piperidine (in DMF) was used as a deprotection agent. The washing steps were performed using DMF. The bromophenol test was used to assess the degree of coupling. Finally, removal of peptide from Rink amide resin and last deprotection was performed using TIS: H<sub>2</sub>O: TFA (1:1:18, v/v) mixture for 3 hours. The peptide was precipitated overnight at -10°C using diethyl ether. After filtration the peptide was solubilized in acetic acid 5% and further lyophilized and stored at -40°C. The phenylalanine pentamer (FFFFF) was also fully investigated at Peptide Institute (Minoh, Osaka, Japan).<sup>48</sup>

### Computer software

The peptides and their various fragments obtained in the MS/MS process were theoretically characterized with the General Protein/Mass Analysis for Window software (GPMW, Lighthouse Data, Denmark). Computer simulation of the 3D structure of peptides performed with the help of the Chem3D Pro 12.0 software.

### CONCLUSIONS

The purity, stability, and molecular weights of small peptides can be evaluated by mass spectrometry. In addition, tandem mass spectrometry (MS/MS) provides detailed information for the structural characterization of peptides, being a method based on the dissociation of ions of interest, which shows the cleavage sites of each peptide molecule as well as the strength and energies of chemical bonds. By electrospray ionization mass spectrometry the time-

dependent decomposition of peptides during storage can be studied and their purity determined. Following purification, the MS spectrum of peptide EEE-OH was found simplified, but its dimer peak increased much. Infrared spectroscopy confirmed the peptide oligomerization. In this work, a pentapeptide, FESNF-NH<sub>2</sub>, was also prepared by stepwise Fmoc methodology using Rink amide resin as a solid support. However, two main peaks appeared in the chromatogram, which were assigned to the pure peptide and its conjugate with a residue from the rink amide linker, due to incomplete cleavage. Fortunately, these compounds separated easily. The arginine residue in the model LWMRFA peptide, introduced in this study for comparison, prevents aggregation because the pI value of the peptide is high at neutral pH and the electrical charge is able to repel individual molecules from each other.

*Acknowledgements.* The authors are indebted to Dr. Gitta Schlosser from the Research Group of Peptide Chemistry, Hungarian Academy of Sciences, Eötvös L. University, Budapest, and Dr. Marilena Manea from the Laboratory of Analytical Chemistry, University of Konstanz, Germany, for their technical support and advises. Funding from Romanian Government under the PN-III-P2-2.1-PED2019-2484 Research Program (Contract PED494, BioPASCAL) of UEFISCDI Bucharest is acknowledged. G.D. thanks for a DAAD fellowship at the University of Konstanz, Germany and for the collaboration with the regretful Prof. Dr. Michael Przybylski.

### REFERENCES

1. S.B.H. Kent, *J. Pept. Sci.*, **2015**, *21*, 136–138.
2. B. Yang, X. Li, C. Zhang, S. Yan, W. Wei, X. Wang, X. Deng, H. Qian, H. Lin and W. Huang, *Org. Biomol. Chem.*, **2015**, *13*, 4551–4561.
3. N.Yadav, M.K. Chauhan and V.S. Chauhan, *Biomat. Sci.*, **2020**, *8*, 84–100.
4. E. Radvar and H.S. Azevedo, *Macromol. Biosci.*, **2019**, *19*, 1800221.
5. L.M.D.L. Rodriguez, Y. Hemar, J. Cornish and M.A. Brimble, *Chem. Soc. Rev.*, **2016**, *45*, 4797–4824.
6. C. Redondo-Gómez, Y. Abdouni, C.R. Becer and A. Mata, *Biomacromolecules*, **2019**, *20*, 2276–2285.
7. D.A.T. Pires, M.P. Bemquerer and C.J. do Nascimento, *Int. J. Pept. Res. Therap.*, **2014**, *20*, 53–69.
8. I. Coin, M. Beyermann and M. Bienert, *Nat. Protoc.*, **2007**, *2*, 3247–3256.
9. K. Nagy-Smith, E. Moore, J. Schneider and R. Tycko, *Proc. Nat. Acad. Sci.*, **2015**, *112*, 9816–9821.
10. A. Lupu, L.M. Gradinaru, V.R. Gradinaru and M. Bercea, *Gels*, **2023**, *9*, 376.
11. B.A. Aggeli, M. Bell, N. Boden, J.N. Keen, P.F. Knowles, T.C.B. McLeish, M. Pitkeathly and S.E. Radford, *Nature*, **1997**, *386*, 259–262.
12. A. Dasgupta, J.H. Mondal and D. Das, *RSC Advances*, **2013**, *3*, 9117–9149.

13. J.M. Carter, Y. Qian, J.C. Foster and J.B. Matson, *Chem. Commun.*, **2015**, 51, 13131–13134.
14. E.D. Eren, G. Tansik, A.B. Tekinay and M.O. Guler, *ChemNanoMat*, **2018**, 4, 837–845.
15. H. Arakawa, K. Takeda, S.L. Higashi, A. Shibata, Y. Kitamura and M. Ikeda, *Polymer J.*, **2020**, 52, 923–930.
16. S. Sutton, N.L. Campbell, A.I. Cooper, M. Kirkland, W.J. Frith and D.J. Adams, *Langmuir*, **2009**, 25, 10285–10291.
17. S. Gupta, I. Singh, A.K. Sharma and P. Kumar, *Front. Bioeng. Biotechnol.*, **2020**, 8, 504.
18. K. Subramani and W. Ahmed, “Self-assembly of proteins and peptides and their applications in bionanotechnology and dentistry”, in “Emerging Nanotechnologies in Dentistry”, William Andrew Publishing, 2012, p. 209–224.
19. A. Kühnle, *Curr. Op. Colloid Interf. Sci.*, **2009**, 14, 157–168.
20. A.P. Chiriac, A. Ghilan, I. Neamtu, L.E. Nita, A.G. Rusu and V.M. Chiriac, *Macromol. Biosci.*, **2019**, 19, 1900187.
21. B.G. Anand, K. Dubey, D.S. Shekhawat and K. Kar, *Sci. Rep.*, **2017**, 7, 1–9.
22. P.W. Frederix, R.V. Ulijn, N.T. Hunt and T. Tuttle, *J. Phys. Chem. Lett.*, **2011**, 2, 2380–2384.
23. M. Muschol, S.E. Hill and M. Mulaj, “Multiple pathways of lysozyme aggregation”, in “Bio-nanoimaging”, Academic Press, 2014, p. 389–396.
24. R. Swaminathan, V.K. Ravi, S. Kumar, M.V.S. Kumar and N. Chandra, *Adv. Prot. Chem. Struct. Biol.*, **2011**, 84, 63–111.
25. R. Gugasyan, I. Vidavsky, C.A. Nelson, M.L. Gross and E.R. Unanue, *J. Immunol.*, **1998**, 161, 6074–6083.
26. S. Zirah, S. Rebuffat, S.A. Kozin, P. Debey, F. Fournier, D. Lesage and J.C. Tabet, *Int. J. Mass Spectrom.*, **2003**, 228, 999–1016.
27. A. Barth and C. Zscherp, *Q. Rev. Biophys.*, **2002**, 35, 369–430.
28. I.W. Hamley, *Angew. Chem. Int. Ed.*, **2014**, 53, 6866–6881.
29. R. Matsumoto, M. Okochi, K. Shimizu, K. Kanie, R. Kato and H. Honda, *Sci. Rep.*, **2015**, 5, 1–9.
30. S.C. Jitaru, A. Neamtu, G. Drochioiu, L. Darie-Ion, I. Stoica, B.A. Petre and V.R. Gradinaru, *Pharmaceutics*, **2023**, 15, 371.
31. C.S. Mocanu, M. Jureschi and G. Drochioiu, *Molecules*, **2020**, 25, 4536.
32. J.M. Schmitter, *J. Chromatogr. A*, **1991**, 557, 359–368.
33. P. Novales-Li, “Human brain acetylcholinesterase”, Doctoral dissertation, University of Oxford, 1993, p. 24–27.
34. H. Tao, S.C. Lee, A. Moeller, R.S. Roy, F.Y. Siu, J. Zimmermann, R.C. Stevens, C.S. Potter, B. Carragher and Zhang, Q. *Nat. Meth.*, **2013**, 10, 759–761.
35. G. Navarra, A. Tinti, M. Leone and V. Militello, *J. Inorg. Biochem.*, **2009**, 103, p.1729–1738.
36. A.F. Dexter, N.L. Fletcher, R.G. Creasey, F. Filardo, M.W. Boehm and K.S. Jack, *RSC Adv.*, **2017**, 7, 27260–27271.
37. C.S. Mocanu, B.A. Petre, L. Darie-Ion, G. Drochioiu, M. Niculaua, I. Stoica, M. Homocianu, L.E. Nita and V.R. Gradinaru, *ChemPlusChem*, **2022**, 87, e202100462.
38. E. Kominami, H. Hoffschulte, L. Leuschel, K. Maier and H. Holzer, *BBA-Enzymol.*, **1981**, 661, 136–141.
39. D.H. Small, Z. Ismael and I.W. Chubb, *Neurosci.*, **1987**, 21, 991–995.
40. S.Z. Hasnain, R. Lourie, I. Das, A.C.H. Chen and M.A. McGuckin, *Immunol. Cell Biol.*, **2012**, 90, 260–270.
41. C.S. Mocanu, L. Darie-Ion, B.A. Petre, V.R. Gradinaru and G. Drochioiu, *J. King Saud Univ. Sci.*, **2022**, 34, 102184.
42. M. Murariu, L. Habasescu, C.I. Ciobanu, R.V. Gradinaru, A. Pui, G. Drochioiu and I. Mangalagiu, *Int. J. Pept. Res. Therap.*, **2019**, 25, 897–909.
43. L. Habasescu, M. Jureschi, B.A. Petre, M. Mihai, R.V. Gradinaru, M. Murariu and G. Drochioiu, *Int. J. Pept. Res. Therap.*, **2020**, 26, 2529–2546.
44. L. Ion, C.I. Ciobanu, M. Murariu, V.R. Gradinaru and G. Drochioiu, *Int. J. Pept. Res. Therap.*, **2016**, 22, 45–55.
45. C.S. Mocanu, B.A. Petre, L. Darie-Ion, G. Drochioiu, M. Niculaua, I. Stoica, M. Homocianu, L.E. Nita and V.R. Gradinaru, *ChemPlusChem*, **2022**, 87, e202100462.
46. P.R. Hansen and A. Oddo, “Fmoc solid-phase peptide synthesis”, in “Peptide antibodies”, Humana Press, New York, NY, 2015, p. 33–50.
47. L. Raibaut, O. El Mahdi and O. Melnyk, *Protein Ligation and Total Synthesis II*, **2014**, 103–154.
48. A. Kagoshima, K. Sekimoto and M. Takayama, *J. Am. Soc. Mass Spectr.*, **2019**, 30, 1592–1600.

